

Mammalian Target of Rapamycin, a Molecular Target in Squamous Cell Carcinomas of the Head and Neck

Panomwat Amornphimoltham,^{1,2} Vyomesh Patel,¹ Akrit Sodhi,¹ Nikolaos G. Nikitakis,^{2,3} John J. Sauk,^{2,3} Edward A. Sausville,³ Alfredo A. Molinolo,¹ and J. Silvio Gutkind¹

¹Oral and Pharyngeal Cancer Branch, National Institute of Dental and Craniofacial Research, NIH, Bethesda; ²Department of Diagnostic Science and Pathology, Dental School; and ³Greenebaum Cancer Center, University of Maryland, Baltimore, Maryland

Abstract

Emerging knowledge on how the dysregulated function of signaling networks contributes to the malignant growth of squamous cell carcinoma of the head and neck (HNSCC) can now be exploited to identify novel mechanism-based anticancer treatments. In this regard, we have observed that persistent activation of the serine/threonine kinase Akt is a frequent event in HNSCC, and that blockade of its upstream kinase, 3'-phosphoinositide-dependent kinase 1, potently inhibits tumor cell growth. Akt promotes cell proliferation by its ability to coordinate mitogenic signaling with energy- and nutrient-sensing pathways that control protein synthesis through the atypical serine/threonine kinase, mammalian target of rapamycin (mTOR). This kinase, in turn, phosphorylates key eukaryotic translation regulators, including p70-S6 kinase and the eukaryotic translation initiation factor, 4E binding protein 1. Indeed, we show here that aberrant accumulation of the phosphorylated active form of S6, the most downstream target of the Akt-mTOR-p70-S6 kinase pathway, is a frequent event in clinical specimens from patients with HNSCC and their derived cell lines. Of interest, this enhanced level of the phosphorylated active form of S6 was rapidly reduced in HNSCC cell lines and HNSCC xenograft models at clinically relevant doses of rapamycin, which specifically inhibits mTOR. Furthermore, we observed that rapamycin displays a potent antitumor effect *in vivo*, as it inhibits DNA synthesis and induces the apoptotic death of HNSCC cells, ultimately resulting in tumor regression. These findings identify the Akt-mTOR pathway as a potential therapeutic target for HNSCC, and may provide the rationale for the early clinical evaluation of rapamycin and its analogues in patients with HNSCC. (Cancer Res 2005; 65(21): 9953-61)

Introduction

Squamous cell carcinoma of the head and neck (HNSCC) is the sixth most common cancer in the developed world, affecting nearly 44,000 patients and resulting in ~ 11,000 deaths each year in the U.S. alone (1). Treatment options are limited and patients with HNSCC frequently fail to respond to standard therapies. Indeed, the 5-year survival rate of patients with advanced HNSCC is <50%, a number that has improved only marginally over the past three decades (2). However, recent advances in the understanding of the molecular

events underlying the initiation, progression, and metastatic spread of HNSCC may expose novel therapeutic targets in HNSCC. Overexpression and/or activity of cell surface receptors, such as those for epidermal growth factor (EGF) and hepatocyte growth factor, EGF receptor (EGFR) and c-Met, respectively, as well as cytokine receptors and G protein-coupled receptors, have been all implicated in the initiation and progression of HNSCCs (3–5). These receptors transduce signals through a variety of biochemical routes that often converge to control the activity of a similar set of intracellular signaling molecules. Among them, accumulating evidence supports a central role for protein kinase B or Akt, a serine/threonine kinase that is stimulated by a multiplicity of cell surface molecules through the activation of phosphoinositide-3-kinases (PI3K) and the consequent stimulation of 3'-phosphoinositide-dependent kinase 1 (PDK1; refs. 6, 7). Akt phosphorylates key signaling molecules, thereby controlling cell cycle progression, cell size, and cell fate decisions, including the activation of cellular programs regulating differentiation, cell survival, or death by apoptosis (6–8). The fact that many frequently occurring activating oncogenic mutations (e.g., in the small GTPase Ras, PI3K, and receptor and nonreceptor tyrosine kinases) result in the constitutive activation of Akt, and that many tumor-suppressor proteins [e.g., PTEN, tuberous sclerosis complex protein 1 and 2 (TSC 1 and 2), and LKB1] act by inhibiting the activity of Akt and its downstream targets, underscores the critical role of the dysregulation of the Akt pathway in cancer (6, 7, 9).

In this regard, we have recently observed that Akt is persistently activated in HNSCC. Indeed, the presence of phosphorylated, active forms of Akt can be readily detected in both experimental and human HNSCCs and in HNSCC-derived cell lines (10). Moreover, blockade of PDK1, which acts upstream of Akt, potently inhibits tumor cell growth (10, 11). Despite accumulating evidence supporting an important role for the Akt pathway in the development of HNSCC, the nature of the biologically relevant pathway(s) through which Akt acts in this tumor type is still unknown. Of interest, recent findings suggest that the ability of Akt to coordinate mitogenic signaling with nutrient-sensing pathways controlling protein synthesis may represent an essential mechanism whereby Akt ultimately regulates cell growth (12, 13). This pathway is initiated by Akt phosphorylation and inactivation of a tumor-suppressor protein, TSC2, which is also known as tuberin (9). TSC2 associates with a second tumor-suppressor protein, TSC1, and act together as a GTPase-activating protein for the small GTPase Rheb1 (9, 14). Thus, inactivation of TSC2 by Akt leads to the accumulation of the GTP-bound (active) form of Rheb1, which in turn promotes the phosphorylation and activation of an atypical serine/threonine kinase known as the mammalian target of rapamycin (mTOR; ref. 15). mTOR then phosphorylates key eukaryotic translation regulators, including p70-S6 kinase (p70S6K) and the eukaryotic translation initiation factor, 4E binding protein 1 (4E-BP1; ref. 16).

Requests for reprints: J. Silvio Gutkind, Oral and Pharyngeal Cancer Branch, National Institute of Dental and Craniofacial Research, NIH, Building 30, Room 212, Convent Drive, Bethesda, MD 20892-4330. Phone: 301-496-6259; Fax: 301-402-0823; E-mail: sg39v@nih.gov.

©2005 American Association for Cancer Research.
doi:10.1158/0008-5472.CAN-05-0921

The latter prevents the repressing activity of 4E-BP1 on the eukaryotic initiation factor 4E (eIF4E), ultimately resulting in enhanced translation from a subset of genes that are required for cell growth (16). Of direct relevance to HNSCC, eIF4E gene amplification and protein overexpression is often associated with malignant progression of this cancer type (17), and its expression levels in surgical margins can predict tumor recurrence (18).

Here, we show that the Akt-mTOR pathway plays a central role in HNSCC. Aberrant accumulation of the phosphorylated active form of S6 (p-S6), the most downstream target of the Akt-mTOR-p70S6K pathway, is a frequent event in clinical specimens from patients with HNSCC and in HNSCC-derived cell lines. We also found that the level of activated S6 was rapidly reduced when HNSCC cell lines were treated with rapamycin, which specifically inhibits mTOR. Furthermore, p-S6 was dramatically reduced in HNSCC xenograft models at clinically relevant doses of rapamycin. Concomitantly, we observed that rapamycin exerts a potent antitumor effect *in vivo*, as it inhibits cell proliferation and induces apoptotic cell death of HNSCC cells, ultimately promoting tumor regression. These findings identify the Akt-mTOR pathway as a potential therapeutic target for HNSCC, thus raising the possibility of exploring the clinical activity of rapamycin and its analogues in patients with HNSCC.

Materials and Methods

Human tissues. Paraffin blocks of formalin-fixed tissues from normal/hyperplastic epithelium ($n = 22$), dysplasias ($n = 20$), and well ($n = 24$), moderate ($n = 23$), and poorly differentiated ($n = 14$) invasive squamous cell carcinomas (SCC) of the oral cavity were retrieved from the archives of the Department of Diagnostic Science and Pathology, Dental School, University of Maryland, with the approval of the Institutional Review Board.

Cell cultures and reagents. HNSCC cell lines HN6, HN8, HN12, HN13, HN30, and HN31 were obtained from Dr. J.F. Ensley (Wayne State University, Detroit, MI) and described previously (19). UMSCC11B was kindly provided by Dr. T. Carey (University of Michigan, Ann Arbor, MI). The human HNSCC cell lines CAL27 and HEp-2 were purchased from the American Type Culture Collection (Manassas, VA). HaCaT cells were derived from normal skin adjacent to a melanoma, and these cells often served as a control, nontumorigenic epithelial cell line (20). All cell lines were grown and maintained in DMEM and 10% fetal bovine serum, penicillin, and streptomycin at 37°C in the presence of 5% CO₂, essentially as described previously (21). HNSCC cell lines were grown to 60% to 70% confluence and then maintained for a further 24 hours in serum-free conditions prior to treatment. For *in vitro* studies, serum-starved cells were treated with rapamycin, LY294002, or AG1478, all purchased from Calbiochem (San Diego, CA), at the indicated concentrations for 30 minutes. Serum-starved cells were also stimulated with 100 ng/mL of EGF for 10 minutes as a positive control. Cells were then harvested, lysed, and proteins subjected to Western blot analysis. For *in vivo* experiments, rapamycin was provided by the Development Therapeutics Program (National Cancer Institute), dissolved in 100% ethanol, and further diluted in an aqueous solution of 5.2% Tween 80 and 5.2% polyethylene glycol immediately before use (22).

Animal studies. All animal studies were carried out according to NIH-approved protocols, in compliance with the Guide for the Care and Use of Laboratory Animals. Female athymic (*nu/nu*) nude mice (Harlan Sprague-Dawley, Frederick, MD), 5 to 6 weeks of age and weighing 18 to 20 g, were used in the study, and housed in appropriate sterile filter-capped cages and fed and watered *ad libitum*. All handling and transplantation procedures were conducted in a laminar-flow biosafety hood.

Establishment and treatment of tumor xenografts in athymic *nu/nu* mice. HN12, CAL27, UMSCC11B, and HEp-2 cells were used to induce HNSCC tumor xenografts in athymic mice as described previously (23). Briefly, exponentially growing cultures were harvested, washed, resuspended in DMEM, and 2×10^6 viable HN12 and UMSCC11B cells or 1×10^7 CAL27

and HEp-2 cells were transplanted s.c. into the left flank of the athymic mice. For tumor growth analysis, tumor weight was determined as described previously (24, 25), whereby tumor volume [$(LW^2/2)$; where L and W represent the length and the width of the tumor] was converted to weight (mg) assuming unit density. The animals were monitored twice weekly for tumor development, and drug treatment was initiated when tumor volume reached ~75 to 250 mg (25, 26). Drug treatment of tumor-bearing animals was essentially as previously described (23). Briefly, for each experiment, tumor-bearing animals were randomly divided into two groups of 20 animals and treated with rapamycin (10 mg/kg/d) or an equal volume of diluent (22). These experiments were repeated thrice. The treatment schedule was a single injection per animal, per day, given i.p., consecutively for 5 days. Animals from each group were euthanized for tissue retrieval at the various time points indicated in the study. The tissues were fixed in 4% buffered paraformaldehyde overnight, dehydrated, and embedded in paraffin using standard protocols, or lysed in protein lysis buffer for Western blot analysis. On completion of the 5-day treatment, the animals were continued to be monitored everyday for tumor growth and body weight. In each case, 1 hour before euthanasia, the mice were injected i.p. with 5-bromo-2-deoxyuridine (BrdUrd; 100 µg/g body weight) for cell proliferation assays (27). Results of animal experiments were expressed as mean \pm SE, and unpaired Student's *t* test was used to determine the difference between treated and control groups for each of the four transplanted cell lines. $P < 0.05$ was considered to be statistically significant.

Immunohistochemistry. The tissue slides were dewaxed in xylene, hydrated through graded alcohols and distilled water, and washed thoroughly with PBS. Antigen retrieval was done using 10 mmol/L citrate buffer (pH 6) in a microwave oven for 20 minutes (2 minutes at 100% power and 18 minutes at 10% power). The slides were allowed to cool down for 30 minutes at room temperature, rinsed twice with PBS, and incubated in 3% hydrogen peroxide in PBS for 30 minutes to quench the endogenous peroxidase. The sections were then washed in distilled water and PBS and incubated in the blocking solution (5% bovine serum albumin in PBS) for 1 hour at room temperature. Excess solution was discarded and the sections incubated with the primary antibody diluted overnight in 1:100 blocking solution at 4°C. After washing with PBS, the slides were sequentially incubated with the biotinylated secondary antibody (Vector Laboratories, Burlingame, CA; 1:300) for 1 hour, followed by the ABC complex (Vector Stain Elite, ABC kit, Vector Laboratories) for 30 minutes at room temperature. The slides were washed and developed in 3,3'-diaminobenzidine (Sigma FASTDAB tablet, Sigma Chemical, St. Louis, MO) under microscopic control. The reactions were stopped by immersing the slides in tap water; the tissues were then counterstained with Mayer's hematoxylin, dehydrated, cleared in xylene, and mounted. Immunohistochemical evaluation was conducted blindly, without knowledge of the clinical and pathologic characteristics of the patients. The p-S6 levels were grouped into three categories based on staining intensity (1, weak staining; 2, moderate staining; and 3, strong staining) and percentage of positive cells according to a previously described scoring method (28). Results were scored by multiplying the percentage of positive cells by the intensity.

Immunocytochemistry. HaCaT cells were grown on the coverslips until 50% confluent, serum-starved, subjected to the different experimental conditions and washed twice in cold PBS. Coverslips were immersed in 100% methanol at -20°C for 10 minutes and washed twice in cold PBS. Blocking step, antibody incubation, and staining conditions were all done as described above. Quenching of the endogenous peroxidase was not necessary, as these cells do not express this enzyme.

Western blotting. Cells were rinsed twice in PBS, lysed with protein lysis buffer [6.25 mmol/L Tris-HCl (pH 6.8), 2% w/v SDS, 10% glycerol, 50 mmol/L DTT], scraped, immediately transferred to microcentrifuge tubes and sonicated for 20 seconds. Protein yield was quantified using the detergent-compatible protein assay kit (Bio-Rad, Hercules, CA). Equivalent amounts of protein (50 µg) were separated by SDS-PAGE and transferred to polyvinylidene difluoride membranes. Equivalent loading was confirmed by staining membranes with Ponceau-S. The membranes were blocked for 1 hour in blocking buffer (5% nonfat dry milk in 0.1% Tween 20-TBS), which was then

replaced by the primary antibody diluted in blocking buffer at the concentration described above, and incubated overnight at 4°C. The membranes were then washed thrice in washing buffer (0.1% Tween 20-TBS). Primary antibody was detected using horseradish peroxidase-linked goat anti-mouse or goat anti-rabbit IgG antibody at 1:4,000 dilution (Santa Cruz Biotechnology, Santa Cruz, CA) and visualized with SuperSignal West Pico chemiluminescent substrate. For Western blot analysis of tissues, small pieces of freshly biopsied xenografts were immediately homogenized in protein lysis buffer, sonicated and subsequently processed as described above.

Antibodies. Rabbit monoclonal anti-phospho-threonine 308-Akt (pT³⁰⁸-Akt), and rabbit polyclonal antiserum against S6, phospho-S6 (p-S6), Akt, phospho-serine 473-Akt (pS⁴⁷³-Akt), 4EBP1, phospho-4EBP1 (p-4EBP1), phospho-tyrosine 1045-EGFR (pY¹⁰⁴⁵-EGFR), and phospho-ERK1/2 (p-ERK1/2) were purchased from Cell Signaling Technology, Beverly, MA. Rabbit polyclonal antiserum against ERK1/2, EGFR, and tubulin were obtained from Santa Cruz; rat monoclonal anti-CD31 was purchased from BD PharMingen, San Diego, CA; and rat monoclonal anti-BrdUrd was obtained from Accurate Chemical, New York, NY. As described above, all antibodies were used for Western blot or immunohistochemistry at a dilution of 1:1,000 and 1:100, respectively.

Terminal nucleotidyl transferase-mediated nick end labeling assay.

The tissue sections were dewaxed in xylene and rehydrated in graded ethanol and distilled water. After washing thrice with PBS, the slides were incubated with proteinase K (Qiagen, Valencia, CA; 20 µg/mL in PBS) for 20 minutes at room temperature, and terminal nucleotidyl transferase-mediated nick end labeling (TUNEL) staining was carried out using the *In situ* Cell Death Detection Kit (Boehringer Mannheim Biochemicals, Indianapolis, IN) according to the manufacturer's instructions.

Statistical analysis. ANOVA followed by the Tukey *t* test were used to analyze the differences between groups after immunohistochemical staining of human HNSCC for phospho-S6 protein. Data analysis was done using GraphPad Prism version 4.00 for Windows, GraphPad Software, San Diego, CA (<http://www.graphpad.com>). *P* < 0.05 was considered statistically significant.

Results

Enhanced levels of p-S6 in human head and neck squamous cell carcinomas. The recent observation that the Akt pathway is persistently activated in most human HNSCCs (10), and the finding that Akt can promote the phosphorylation of the ribosomal S6 protein through mTOR, thereby controlling cell growth through increased mRNA translation (22), prompted us to explore whether HNSCC exhibit increased levels of the phosphorylated form of S6. Initially, we confirmed that p-S6 could be detected in epithelial cells, and that its accumulation correlates with the activation of the PI3K-Akt pathway. Using an immortalized human epidermal cell line, HaCaT, we observed that the treatment with EGF (100 ng/mL, 10 minutes), which activates Akt as judged by its phosphorylation of threonine 308 (pT³⁰⁸-Akt) and serine 473 (pS⁴⁷³-Akt), increases the immunodetection of p-S6 without affecting its total expression level (Fig. 1A). The requirement of the PI3K-Akt pathway for S6 phosphorylation was further documented by the disappearance of the band corresponding to p-S6 on pretreatment with LY294002 (50 µmol/L, 30 minutes), a selective PI3K inhibitor (29) which also decreased the phosphorylation of S6 caused by EGF. Similarly, treatment with EGF resulted in a strong immunocytochemical cytoplasmic reactivity for p-S6 in HaCaT (Fig. 1B), which was diminished by LY294002. These results are aligned with the ability of PI3K-Akt-mTOR pathway to control the phosphorylation of S6, and indicate that the accumulation of p-S6 correlates with the activity of the Akt-initiated signaling route.

We then examined the phosphorylation status of S6 in a large panel of HNSCC-derived cell lines by Western blot analysis using anti-p-S6 antibodies. These experiments revealed that most HNSCC cells lines exhibit high levels of p-S6, which persisted even after

serum and growth factor deprivation (Fig. 1C). The single exemption was HN13, which still retained the ability to stimulate S6 phosphorylation in response to EGF. Because EGFR represents an extensively studied molecular target in HNSCC (3, 30), we evaluated the contribution of EGFR to the elevated activity of the mTOR pathway in these HNSCC cells lines. Of interest, in a prior study, we have documented that some HNSCC cell lines (but not others) exhibit elevated basal EGFR activity (21). Using HN12 as an example of a cell line displaying active EGFR, we observed that AG1478, a potent EGFR inhibitor, decreased the basal level of tyrosine-phosphorylated EGFR, which was paralleled by a marked reduction in the phosphorylated species of ERK1/2 (Fig. 1D). AG1478 also diminished the accumulation of p-S6, albeit at concentrations slightly higher than those required to inhibit EGFR and ERK1/2 (Fig. 1D). In contrast, the status of phosphorylation of S6 was not affected by the treatment with AG1478 in HEp-2 cells, as an example of a HNSCC cell line that does not display elevated EGFR activity (Fig. 1D). As internal controls, EGF provoked a remarkable increase in pY¹⁰⁴⁵-EGFR, whereas LY294002 decreased p-S6 levels in both cell lines. Unexpectedly, LY294002 caused a variable increase in p-ERK1/2, an observation that warrants further investigation. We can conclude that both EGFR-dependent and -independent mechanisms can contribute to the elevated activity of the mTOR pathway in HNSCC cell lines.

We next took advantage of the availability of this immunodetection system for p-S6 to investigate the status of activation of the mTOR pathway in tissues. Indeed, immunohistochemical analysis of p-S6 revealed that human HNSCC exhibits a pattern of expression of p-S6 similar to that of active Akt, which correlated with disease progression. p-S6 immunoreactivity was limited to very few cells in normal squamous epithelia, whereas the number of cells and intensity of the staining pattern increased in hyperplasias (Fig. 2A). The staining in both cases was restricted to the suprabasal layers. Conversely, dysplasias showed a remarkably higher degree of reactivity, and many of them displayed either a scattered or uniformly strong staining in the basal and parabasal cell layers, a feature that was not observed in nondysplastic tissue (Fig. 2A). Invasive squamous carcinomas disclosed variable cytoplasmic p-S6 staining, with more differentiated tumors showing, in general, a higher intensity of immunostaining as well as a higher number of positive cells. (Fig. 2B and C). In many tumors, the p-S6 immunoreactivity was more noticeable along the invasive borders of the neoplasia, regardless of their degree of differentiation (Fig. 2B). Cancer cell strands invading the stroma tended to display more p-S6 immunoreactivity than the rest of the tissue (Fig. 2B). When a large tissue sample collection was analyzed, significant differences in the percentage and intensity of positively stained cells were observed between normal and dysplastic tissue (*P* < 0.001), well-differentiated SCC (*P* < 0.001), moderately differentiated SCC (*P* < 0.001), or poorly differentiated SCC (*P* < 0.05), supporting the notion that p-S6 accumulation may represent an early event in the carcinogenesis process.

Rapamycin inhibits the Akt-mTOR-S6 signaling pathway in head and neck squamous cell carcinoma cells. In agreement with the likely link between the increased enzymatic activity of Akt and the phosphorylation of mTOR, preventing the activation of Akt by PI3K and PDK1 inhibitors, LY294002 and UCN-01 (31, 32), respectively, diminished the phosphorylation of S6, as shown in Fig. 3A using HN12 cells, as an example. p-S6 was also drastically reduced by the exposure of these cells to a selective mTOR inhibitor, rapamycin (33), which did not affect the expression level of S6 (Fig. 3A). As expected, the level of p-Akt did not change when

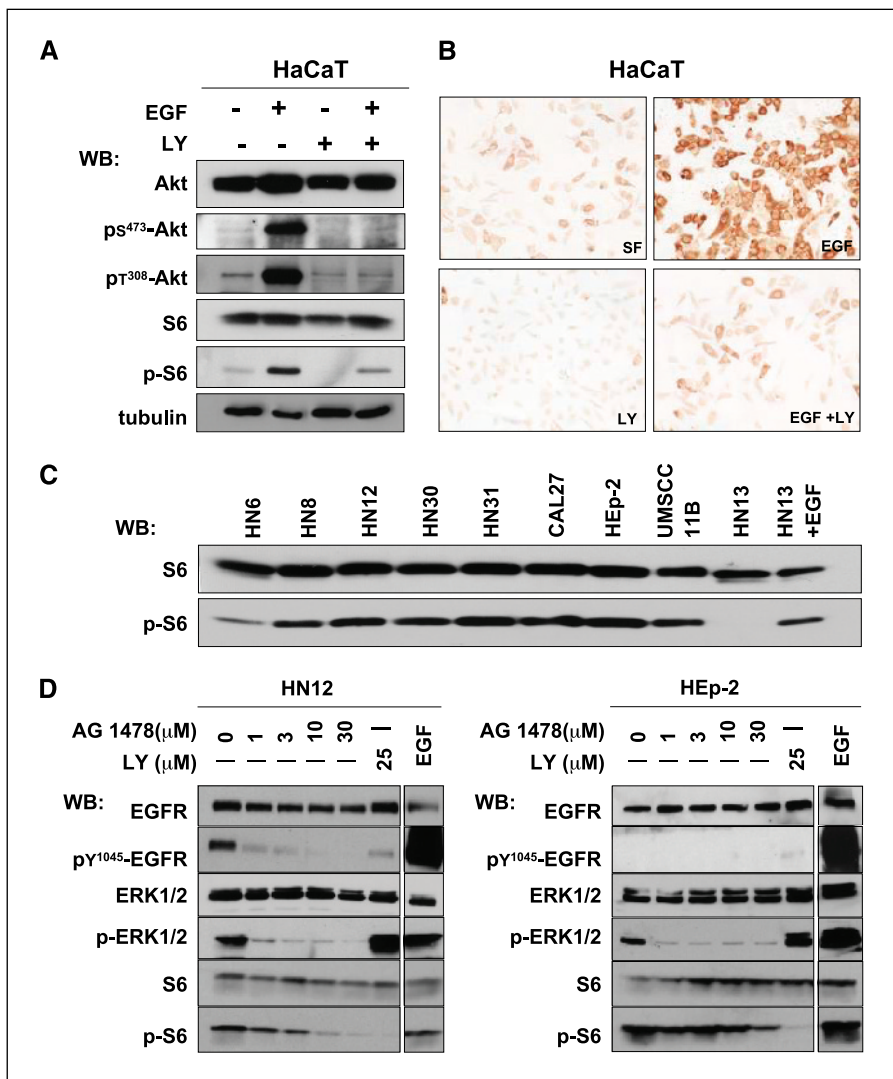


Figure 1. A, Western blot (WB) analysis of Akt and S6 protein expression in human epithelial cells. Serum-deprived HaCaT cells were treated with LY294002 (LY; 50 μ M/L for 30 minutes) or vehicle and then with EGF (100 ng/mL for 10 minutes), as indicated. Total Akt and S6 protein as well as their phosphorylated forms including Akt phosphorylated in threonine 308 (pT³⁰⁸-Akt) and serine 473 (ps⁴⁷³-Akt) and phosphorylated S6 (p-S6) were detected in whole cell lysates. The accumulation of p-Akt and p-S6 were strongly induced by EGF, but inhibited upon treatment with LY294002. B, detection of p-S6 by immunocytochemistry in HaCaT cells cultured on coverslips and treated as in (A); the cells were fixed in 100% methanol (-20° C for 10 minutes) and p-S6 detected as described in Materials and Methods. Cells treated with EGF exhibit strong cytoplasmic immunoreactivity to p-S6. In contrast, cells treated with LY294002 show weaker cytoplasmic staining, even when treated with EGF, comparable to its basal level in serum-free condition (SF). C, Western blot analysis of p-S6 in a panel of HNSCC cell lines. Cell lysates were harvested from serum-deprived HNSCC cells lysed and resolved as described in Materials and Methods. Immunoblotting for phosphorylated (p-S6) and total S6 were done in the same filter after stripping the membrane. Where indicated, cells were treated with EGF (100 ng/mL for 10 minutes). D, EGFR-dependent and -independent activation of p-S6 in HNSCC cell lines. Western blot analysis of total and phosphorylated form of EGFR, ERK1/2, and S6 proteins from cell lysates of representative HNSCC cell lines treated with EGFR inhibitor (AG1478) at the indicated concentrations or with LY294002 (LY; 50 μ M/L) for 30 minutes. Where indicated, cells were stimulated with EGF (100 ng/mL for 10 minutes). Of note, in HN12 cells (left) the inhibition of p-EGFR and p-ERK1/2 was observed at very low concentration of AG1478 (1 μ M/L), whereas the accumulation of p-S6 activity was inhibited \sim 50% at 10 μ M/L of this inhibitor. No changes were observed in the total protein levels. HEp-2 cells (right) have very low EGFR activity, and >30 μ M/L of AG1478 is required to inhibit \sim 50% of p-S6 levels.

cells were exposed to rapamycin, thus supporting the known specificity of this therapeutic agent. This inhibition of p-S6 accumulation was dose-dependent, achieving a maximal response even at low nanomolar concentrations. Of interest, rapamycin also decreased the phosphorylation of 4E-BP1, another target of the mTOR pathway (34), albeit at slightly higher concentrations than those required to decrease the phosphorylation of S6.

Rapamycin exhibits potent antitumor properties against head and neck squamous cell carcinoma tumor xenografts.

Based on the aberrantly high activity of the Akt-mTOR-S6 pathway in HNSCC, we evaluated the potential benefit of inhibiting mTOR for the treatment of this aggressive tumor type. For these studies, athymic *nu/nu* mice bearing human HN12 cell xenografts, a previously described HNSCC model (23), were injected i.p. for 5 consecutive days with either rapamycin (10 mg/kg/d) or vehicle, and tumor growth was monitored for up to 20 days after the initial treatment. A potent antitumor effect of rapamycin became apparent as early as 3 days after treatment initiation (Fig. 3B and C), and this effect was sustained over the course of the study. At the end of the study (day 20; Fig. 3D), there was a statistically significant difference ($P < 0.0001$) between the vehicle-treated tumors, which weighed an average of 854 ± 144 mg, a $>300\%$ increase over their weight on day 1 (220 ± 29 mg), and the

rapamycin-treated group, which showed a marked growth inhibition over the same period, with an average tumor weight of 105 ± 21 mg, nearly half of their weight before the treatment (206 ± 30 mg). In fact, within 10 days after the initiation of the rapamycin treatment, 30% of the animals displayed complete tumor remission, whereas in the rest of the animals, rapamycin halted tumor growth; both phenomena lasted beyond 60 days, a time point at which no control-treated animals survived. We next took advantage of the ability of HEp-2, CAL27, and UMSSC11B cell lines to form tumors when injected in athymic *nu/nu* mice (35–37) to extend this analysis to other human HNSCC xenograft models. As shown in Fig. 3E–G, we observed a highly significant decrease in the growth of all HNSCC tumor models tested following a 5-day rapamycin administration scheme similar to that used for HN12 xenografts. Particularly, CAL27 and UMSSC11B xenografts were very sensitive to rapamycin, observing lack of further tumor growth for an extended observation period (>50 days). The only exceptions among all treated groups were the animals bearing HEp2 xenografts (Fig. 3G), 20% of which exhibited a partial tumor regrowth 2 weeks after a single cycle of rapamycin treatment. Nonetheless, these tumors grew much slower than in vehicle-treated animals therein. Student's *t* test analysis of the data revealed that the difference between the rapamycin-treated and

control group were highly significant at day 20 ($P < 0.0020$ for CAL27, $P < 0.0021$ for UMSCC11B, and $P < 0.0022$ for HEP-2). Drug toxicity, as assessed by weight loss, was not significant. Collectively, these results suggested that the administration of rapamycin at tolerable doses causes a potent antitumor effect in HNSCC tumor xenografts after only one cycle of administration.

Rapamycin causes a dramatic reduction in the levels of p-S6 in head and neck squamous cell carcinoma xenografts. Based on the antitumoral effects of rapamycin in HNSCC xenografts, we next explored whether the effects of this potential therapeutic agent were reflected by a decrease in p-S6 *in vivo*. As shown in Fig. 4A, when lysates obtained from HN12 xenografts at the indicated times were examined by Western blotting, a clear reduction in the accumulation of p-S6 without any consistent variation in the total level of S6 was readily detectable as early as 1 day after treatment. Furthermore, this biochemical consequence of rapamycin treatment was even more clearly displayed by the parallel immunohistochemical analysis of these tumor xenografts. Indeed, as shown in Fig. 4B, striking differences between the control and the treated group could be observed throughout the treatment. For example, on day 2 (Fig. 4B, top) almost 90% of the cells in the tumors growing in vehicle-treated mice displayed strong cytoplasmic immunoreactivity for p-S6, but <20% were positive in the rapamycin-treated tumors. Similar results were observed in tissues excised on days 5 and 10 (Fig. 4B, bottom), the latter 5 days after the last day of treatment, paralleling the detection of p-S6 by Western blot analysis (Fig. 4B, top) that served as a quantitative approach.

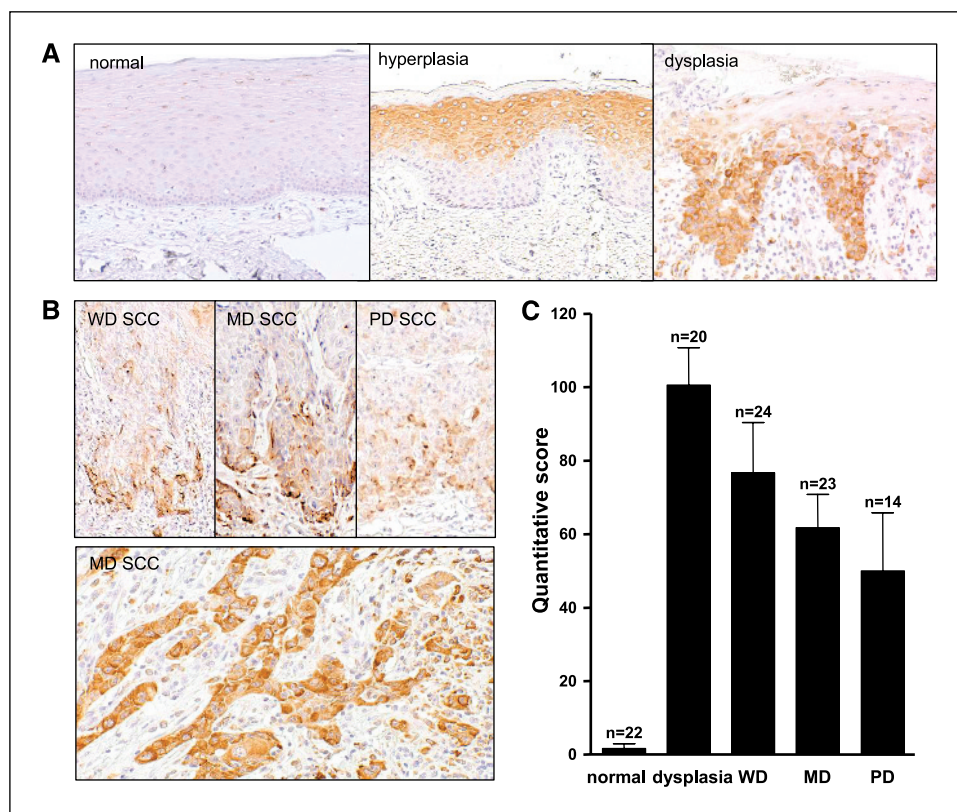
Rapamycin inhibits DNA synthesis and triggers head and neck squamous cell carcinoma cell apoptosis *in vivo*. The striking antitumor activity of rapamycin in HNSCC xenografts raised the question as to what is the nature of the biological events triggered by the treatment with rapamycin in this *in vivo* model.

Of note, lysates from HN12 tumors excised 2 to 3 days after the initiation of the treatment often exhibited signs of protein degradation or cleavage (i.e., see tubulin Western blot; Fig. 4A), and the corresponding tissues displayed lower cellular density (Fig. 4B, top), both consistent with intratumoral cell death. Thus, we explored whether the treatment with rapamycin could promote apoptosis in HNSCC cells. Interestingly, by using an *in situ* TUNEL assay, we consistently observed that between days 2 and 3, there was a large increase in the number of apoptotic nuclei in tumors treated with rapamycin when compared with the vehicle-treated controls (Fig. 5A). However, there were no marked differences in the number of apoptotic cells thereafter (data not shown). Instead, we observed a clear reduction in DNA synthesis. As shown in Fig. 5B, xenografts from rapamycin-treated animals exhibit a lower number of BrdUrd immunoreactive nuclei during the course of the rapamycin treatment. This cytostatic effect persisted even after the completion of the rapamycin administration (data not shown). We also evaluated the differences in vascularization between rapamycin- and vehicle-treated animals. As shown in Fig. 5C, the immunohistochemical staining of blood vessels with the endothelial cell antigen CD31 showed that rapamycin-treated tumors display a less dense vascular network, as evident from the reduced number of cross-sectioned vessels, as compared with tumors growing in mice injected with vehicle. Thus, rapamycin treatment promotes the rapid apoptotic death of HNSCC cells, and a prolonged inhibition of the proliferative capacity of the remaining tumor cells concomitant with a reduction in tumor vascularity.

Discussion

Remarkable progress has been made in the elucidation of the genetic and epigenetic events by which the sequential accumulation of alterations in oncogenes and tumor suppressor genes and their

Figure 2. A and B, immunohistochemical detection of activated S6 in human oral epithelium and HNSCC. A, in normal oral mucosa (left), only a few isolated squamous cells exhibit mild p-S6 staining. However, in the hyperplastic epithelium (middle) ~60% of the squamous cells show p-S6 immunoreactivity with moderate intensity. The reactivity is still confined to the suprabasal layers. About 50% of the cells disclose moderate to strong immunoreactivity in severe dysplasia (right). Frequently, in advanced preneoplastic lesions, the basal and parabasal layers were strongly positive for p-S6 (right). Note that isolated inflammatory cells (right), also show intense immunoreactivity. B, well, moderately, and poorly differentiated squamous cell carcinomas of head and neck (WD, MD and PD SCC, respectively), display strong immunoreactivity in the malignant cells, particularly along the invasive border of the neoplasia. Isolated SCC cells or a narrow strand of neoplastic cells tend to be strongly positive for p-S6, regardless of the degree of differentiation of the tumor (bottom). C, quantitative analysis of immunohistochemistry: data represents the scores resulting from multiplying the percentage of positive cells by the intensity of positively staining cells (scored as 1, 2, or 3, as described in Materials and Methods) observed in normal/hyperplastic, dysplasia, well differentiated (WD), moderately differentiated (MD), and poorly differentiated (PD) squamous carcinoma (SCC). The number of cases (n) analyzed is indicated.



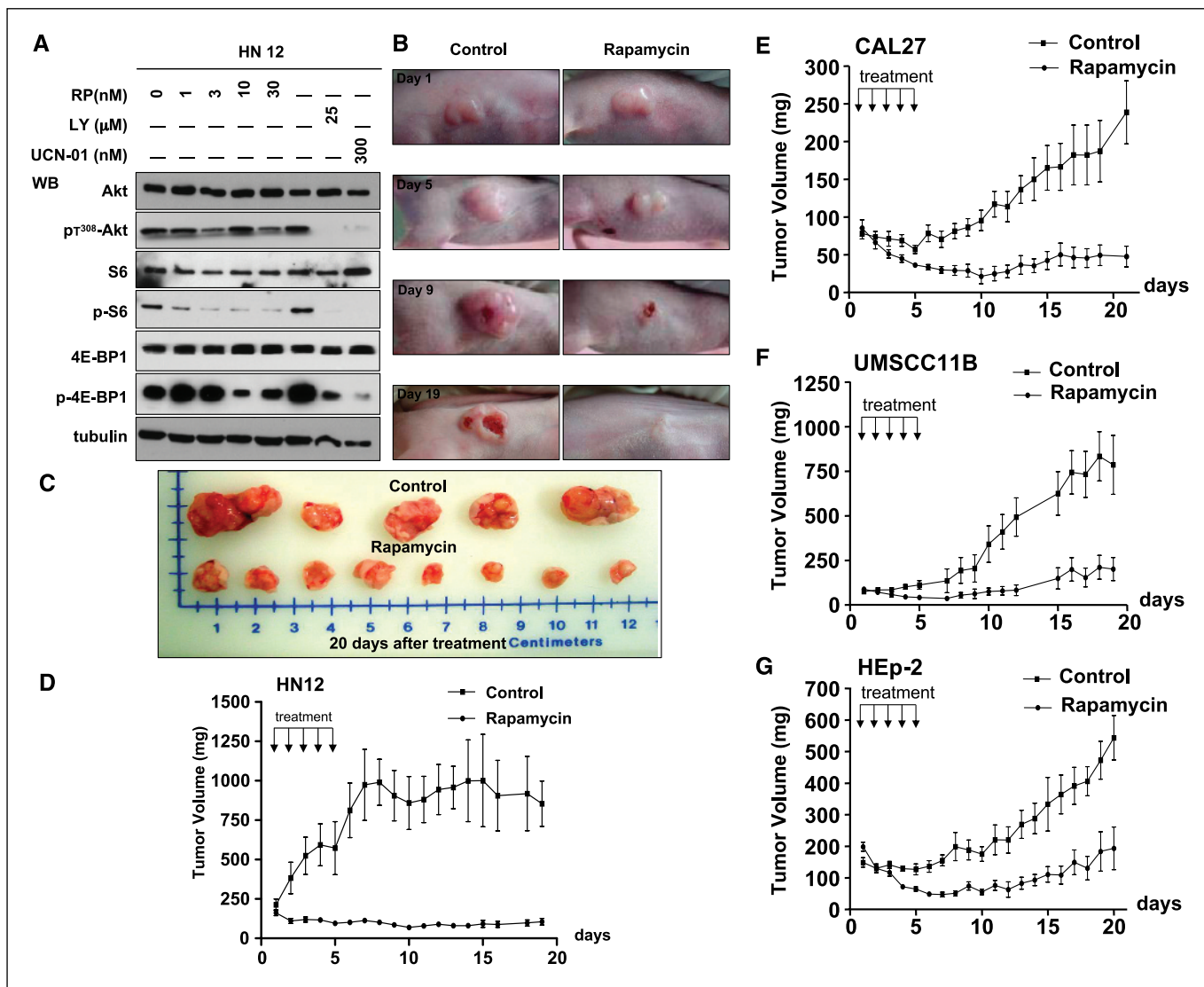


Figure 3. A, constitutively phosphorylated S6 in HNSCC cells is inhibited by rapamycin. Western blot analysis of total Akt, S6, and 4E-BP1, and their phosphorylated forms; pT³⁰⁸-Akt, p-S6, and p-4E-BP1 was done in HN12 treated with rapamycin at the indicated concentration for 30 minutes. Inhibition of p-S6 and p-4E-BP1 was achieved even at low nanomolar concentrations, whereas no changes were observed in their total protein expression. The Akt pathway was blocked by UCN-01 and LY294002, which act on PDK1 and PI3K, respectively, and thus served as controls. B, tumor regression observed in HNSCC xenografts treated with rapamycin. HN12 cells were used to establish xenografts in athymic *nu/nu* mice, and tumor-bearing animals were treated i.p. for 5 consecutive days (i.p./q.d. × 5) with either rapamycin (10 mg/kg; *n* = 20) or an equivalent volume of 5.2% Tween 80 and 5.2% polyethylene glycol buffer (control; *n* = 20). An example of tumor regression in rapamycin-treated animals is depicted. C, lesions dissected from HN12 xenograft 20 days after treatment with rapamycin or vehicle control. D, tumor size from HN12 xenograft in both rapamycin- and vehicle-treated groups was assessed daily, as indicated, and tumor weight was calculated as described in Materials and Methods. Points, mean tumor weight (mg); bars, ± SE. Student's *t* test was used to determine the difference between the rapamycin-treated and control groups (*P* < 0.0001) at day 20. Data are from a representative experiment that was repeated thrice with similar results. Similar analysis was done in animals bearing CAL27 (E), UMSSC11B (F), and HEP-2 (G) HNSCC tumor xenografts. Mean tumor weight (mg) in vehicle (Control) and rapamycin-treated groups are depicted.

related protein products enable HNSCC progression (4, 5). Concurrent advances in our understanding of how the aberrant function of signaling networks contributes to tumor cell growth can now also be exploited for the identification of novel mechanism-based anticancer treatments. In this regard, deregulated expression and activity of EGFR and c-Met (38, 39), overexpression of PI3K (40), persistent activation of the transcription factors nuclear factor κ B and signal transducers and activators of transcription 3/5 (41, 43), and the Akt signaling pathway (10), among others, are frequently observed in HNSCC. These observations have provided the molecular basis for current efforts exploring the clinical benefits of targeting these pathways in patients with advanced HNSCC (44, 45). Building on the observations that experimental and human HNSCC

exhibit aberrantly active Akt, and that mTOR is hyperphosphorylated in HNSCC cell lines (10), we explored here whether the Akt-mTOR pathway was overactive in HNSCC. Indeed, by evaluating the status of phosphorylation of the ribosomal protein S6, a well-known downstream target of mTOR, we observed that the mTOR-p70S6K-S6 pathway is persistently activated in early dysplastic lesions, and that this overactivity persists during tumor progression. Furthermore, we observed that this pathway can be inhibited *in vitro* and *in vivo* by rapamycin, which results in rapid tumor regression concomitant with a marked decrease in cell proliferation, enhanced apoptosis, and reduced tumor vascularity, thus suggesting that mTOR may represent a suitable target for pharmacologic intervention in HNSCC.

The precise mechanism by which the blockade of mTOR by rapamycin exerts such a potent antitumor effect is, at present, not fully understood. As for the wide variety of murine and human cancer cells (46, 47), exposure of a panel of HNSCC cell lines to rapamycin *in vitro* reduced cell cycle progression, particularly by delaying their entry into S phase, and by arresting cell lines in G₁ phase at high doses (data not shown). Thus, rapamycin was expected to be cytostatic, and to reduce or delay tumor growth. Instead, we observed a dramatic biological effect *in vivo*, including the apoptotic death of the HNSCC cells, and the consequent collapse of the tumor architecture and its rapid regression. Furthermore, in the vast majority of the cases analyzed, we did not observe tumor regrowth even after an extended observation period (50-60 days) after the end of the treatment cycle. Although rapamycin may elicit an

antiangiogenic response that deprives cancer cells from their oxygen and nutrient supply (48, 49), it is unclear whether the reduction in tumor vascularity is responsible for its potent antitumor effects or whether, instead, the decrease in the vascular network may represent a direct consequence of the rapid reduction in the size of the rapamycin-treated tumors. Another possible explanation is that the role of mTOR in cell growth and survival *in vivo* may not be reflected under conventional *in vitro* culturing conditions. In this regard, mTOR sits at the crossroad of a network of molecular pathways sensing the energy supply, the exposure to growth-promoting or inhibitory factors, the metabolic status of the cells, and the availability of nutrients, and integrates this complex array of incoming information to regulate the synthesis of proteins that are required for cell growth (50). Thus, we can speculate that whereas under culturing conditions, mTOR may not be strictly required for cell growth, tumor cells may have become dependent on the activity of mTOR to overcome the growth-inhibitory and anti-survival effect of the restricted availability of nutrients, oxygen, and energy sources encountered by cancer cells in the tumor microenvironment.

Whereas no activating mutations have yet been described in mTOR, this kinase can be persistently activated by the aberrant function of growth factor receptors and their downstream targets. In particular, HNSCC tends to express high levels of EGFR, and overexpression and activity of this growth factor receptor often correlates with poor clinical outcome (51). This led to a number of current clinical efforts aimed at inhibiting EGFR as a molecular targeted approach to treat patients with HNSCC (3, 30, 52). Of interest, whereas in some HNSCC cell lines, EGFR inhibition did not affect the activity of the mTOR pathway, in others, a reduction in the status of phosphorylation of S6 after EGFR blockade was observed, albeit often requiring high concentrations of EGFR inhibitors. These findings may have important clinical implications, as they may provide a mechanistic framework for using molecules interfering with mTOR function in combination with EGFR inhibitors, depending on the interplay between the mTOR pathway and EGFR activity in individual HNSCC patients.

mTOR could also be activated by genetic or epigenetic inactivation of molecules that act as negative regulators of the mTOR pathway (50). Among them, several tumor suppressor gene products, including phosphatase and tensin homologue (PTEN), a phosphatidylinositol-3-phosphatase that is inactivated in a number of rare autosomal-dominant cancer-related syndromes such as Cowden syndrome and in a variety of frequent human malignancies such as glioblastomas, endometrial, breast, prostate, and colon cancers (53, 54); LKB1, a protein kinase that is inactivated in Peutz-Jeghers cancer-prone syndrome (9, 55); and the TSC1 and TSC2 complex that acts as a Rheb1 GTPase-activating protein, which are mutated in tumor-prone tuberous sclerosis patients (9, 56), all encode proteins that converge to inhibit the activation of mTOR. Of interest, emerging evidence suggests that these tumors are particularly sensitive to rapamycin and its derivatives (9). In this regard, although mutations in *pten* have been described with only low incidence in HNSCC, epigenetic events resulting in the decreased expression of PTEN are often observed in HNSCC (57). In addition, we have recently found that HNSCC exhibit a decreased expression of LKB1,⁴ which, together with the frequent overactivity of EGFR (38), gene amplification and overexpression of the 110 subunit of PI3K- α (40), and the persistent activation of Akt (10), may contribute to the high

⁴ Unpublished results.

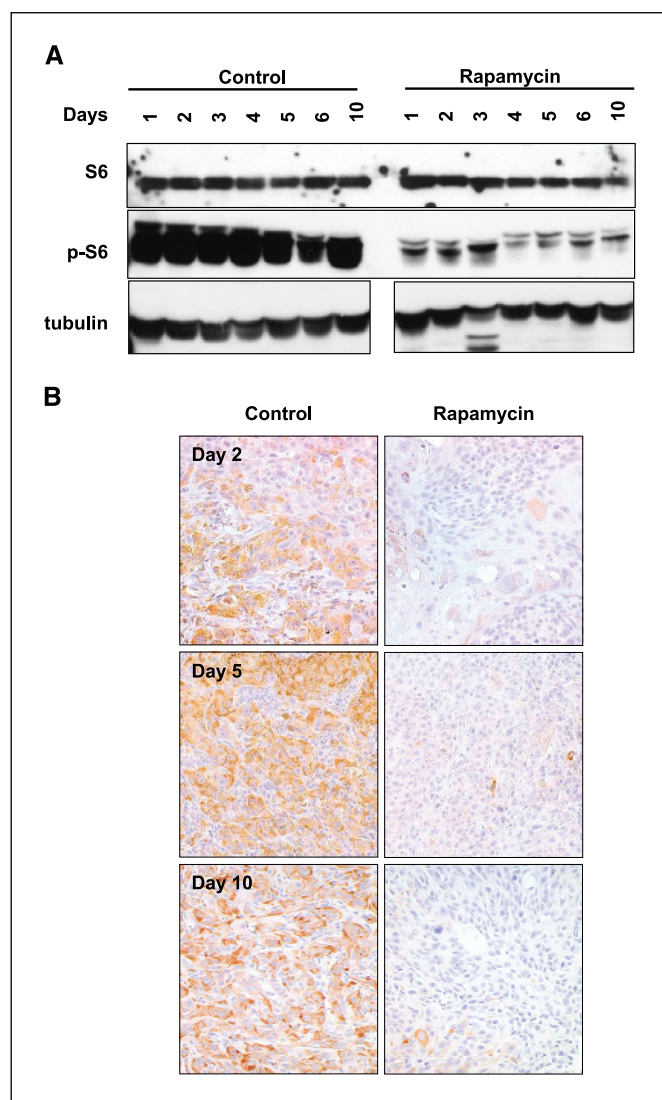


Figure 4. A, Western blot analysis of total and phosphorylated S6 protein in tissue lysates from HN12 xenograft treated with rapamycin or vehicle at the indicated days. A reduction in p-S6 expression level was observed immediately after the first day of treatment, without changes in total S6. Tubulin was used as loading control. B, examples of p-S6 immunostaining in xenograft tumors (days 2, 5, and 10). Paralleling the immunoblot analysis, the rapamycin-treated tumors show only a few positively stained cells, whereas 90% of tumor cells in vehicle control tissues show strong cytoplasmic immunoreaction to p-S6. Similar results were obtained in HEP-2, CAL27, and UMSSC11B tumor xenografts (data not shown).

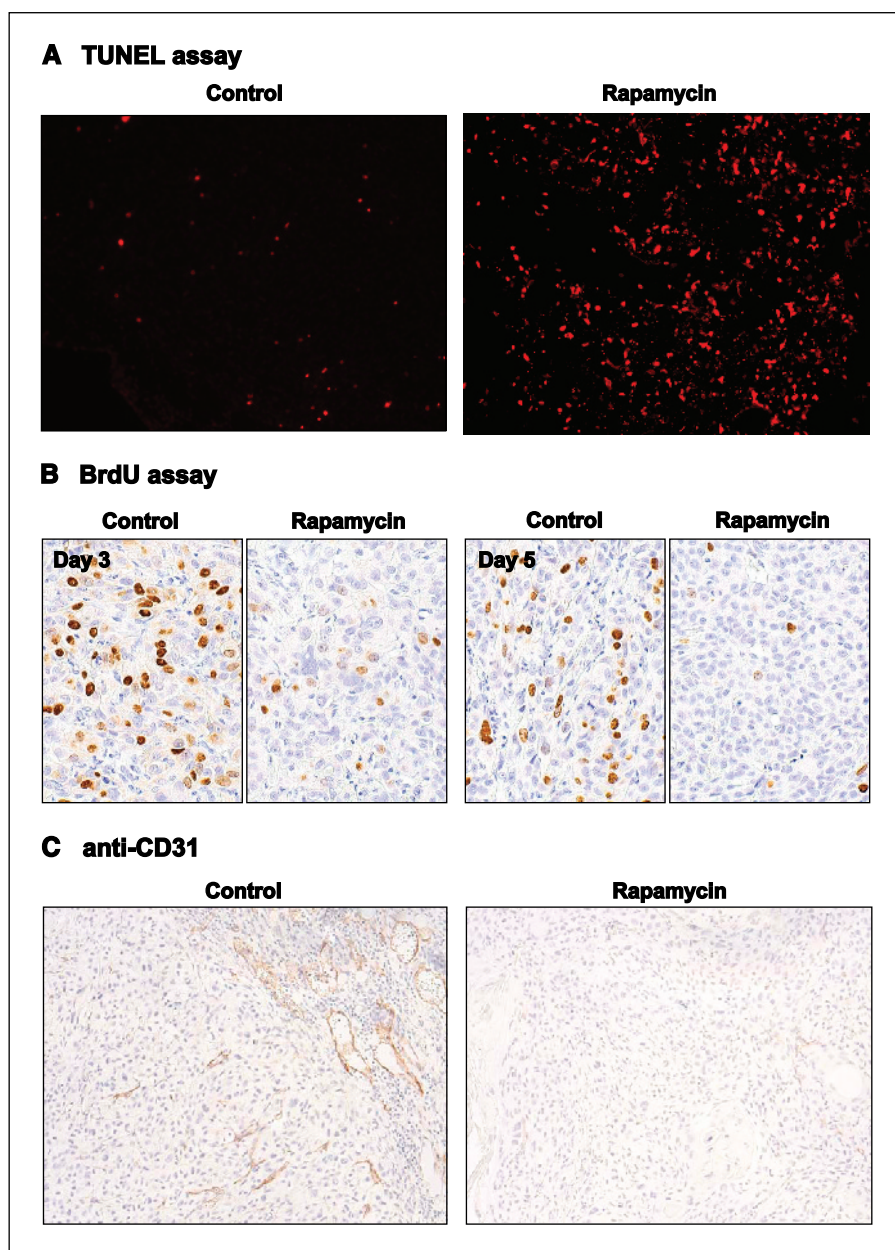


Figure 5. A, TUNEL assay in tumor tissues from HN12 xenograft model. A higher number of apoptotic nuclei is readily observed in tumors from rapamycin-treated mice at day 2, as compared with control animals. B, BrdUrd immunostaining in xenograft tissues. Whereas a high number of positively BrdUrd stained cells is seen in vehicle-treated tumors on both days 3 and 5, fewer immunoreactive cells are detected in tumor tissues from rapamycin-treated animals, which is indicative of a decreased DNA synthesis. C, immunohistochemistry for CD31, an endothelial cell marker, shows remarkable reduction in the number of blood vessels in HNSCC xenografts from mice treated with rapamycin for 5 days as compared with dense vascular networks in the tumors obtained from animals treated with vehicle control.

activity of mTOR in HNSCC. This, in turn, may sensitize tumor cells to the antiproliferative and proapoptotic effect of rapamycin.

The recent clinical evaluation in phase I trials of rapamycin derivatives, including CCI779 and RAD001, revealed that these novel anticancer agents display encouraging antitumor activity with minimal toxicity and no immunosuppression over a broad range of dose levels (46, 58, 59). Based on these promising results, rapamycin and its derivatives are now being actively evaluated for their clinical activity against a wide range of frequent human malignancies, with particular emphasis on those that exhibit deregulated activity of mTOR (47, 60). Thus, the results presented in this report indicating that the activation of mTOR pathway is an early event in squamous carcinogenesis and that its inhibition by rapamycin exerts potent antitumor effects in preclinical models of HNSCC, suggest that rapamycin and its derivatives may represent attractive candidates—either alone or in combination with other chemotherapeutic agents—for the treatment of this aggressive

cancer. Furthermore, determination of the phosphorylation status of S6 by immunohistochemical evaluation of tumor or surrogate tissues may help in establishing the effectiveness of these treatments in blocking the mTOR pathway in patients with HNSCC, thus providing a readily available molecular end point to monitor the treatment efficacy. Together, these data and the lack of effective treatment strategies in patients with advanced HNSCC may provide the rationale for the early assessment of the use of rapamycin and its derivatives as a mechanism-based therapeutic approach for the treatment of patients with refractory squamous carcinomas of the head and neck.

Acknowledgments

Received 3/21/2005; revised 8/1/2005; accepted 8/30/2005.

The costs of publication of this article were defrayed in part by the payment of page charges. This article must therefore be hereby marked *advertisement* in accordance with 18 U.S.C. Section 1734 solely to indicate this fact.

References

1. Jemal A, Murray T, Ward E, et al. Cancer statistics, 2005. *CA Cancer J Clin* 2005;55:10–30.
2. Jemal A, Clegg LX, Ward E, et al. Annual report to the nation on the status of cancer, 1975–2001, with a special feature regarding survival. *Cancer* 2004;101:3–27.
3. Forastiere A, Koch W, Trotti A, Sidransky D. Head and neck cancer. *N Engl J Med* 2001;345:1890–900.
4. Mao L, Hong WK, Papadimitrakopoulou VA. Focus on head and neck cancer. *Cancer Cell* 2004;5:311–6.
5. Hunter KD, Parkinson EK, Harrison PR. Profiling early head and neck cancer. *Nat Rev Cancer* 2005;5:127–35.
6. Brazil DP, Yang ZZ, Hemmings BA. Advances in protein kinase B signalling: AKTion on multiple fronts. *Trends Biochem Sci* 2004;29:233–42.
7. Luo J, Manning BD, Cantley LC. Targeting the PI3K-Akt pathway in human cancer: rationale and promise. *Cancer Cell* 2003;4:257–62.
8. Lawlor MA, Alessi DR. PKB/Akt: a key mediator of cell proliferation, survival and insulin responses? *J Cell Sci* 2001;114:2903–10.
9. Inoki K, Corradetti MN, Guan KL. Dysregulation of the TSC-mTOR pathway in human disease. *Nat Genet* 2005;37:19–24.
10. Amornphimoltham P, Sriuranpong V, Patel V, et al. Persistent activation of the Akt pathway in head and neck squamous cell carcinoma: a potential target for UCN-01. *Clin Cancer Res* 2004;10:4029–37.
11. Patel V, Lahusen T, Leethanakul C, Igishi T, et al. Antitumor activity of UCN-01 in carcinomas of the head and neck is associated with altered expression of cyclin D3 and p27(KIP1). *Clin Cancer Res* 2002;8:3549–60.
12. Shamji AF, Nghiem P, Schreiber SL. Integration of growth factor and nutrient signaling: implications for cancer biology. *Mol Cell* 2003;12:271–80.
13. Sekulic A, Hudson CC, Homme JL, et al. A direct linkage between the phosphoinositide 3-kinase-AKT signaling pathway and the mammalian target of rapamycin in mitogen-stimulated and transformed cells. *Cancer Res* 2000;60:3504–13.
14. Inoki K, Li Y, Xu T, Guan KL. Rheb GTPase is a direct target of TSC2 GAP activity and regulates mTOR signaling. *Genes Dev* 2003;17:1829–34.
15. Manning BD, Cantley LC. Rheb fills a GAP between TSC and TOR. *Trends Biochem Sci* 2003;28:573–6.
16. Hay N, Sonenberg N. Upstream and downstream of mTOR. *Genes Dev* 2004;18:1926–45.
17. Sorrells DL, Meschonat C, Black D, Li BD. Pattern of amplification and overexpression of the eukaryotic initiation factor 4E gene in solid tumor. *J Surg Res* 1999;85:37–42.
18. Nathan CA, Amirghahri N, Rice C, Abreo FW, Shi R, Stucker FJ. Molecular analysis of surgical margins in head and neck squamous cell carcinoma patients. *Laryngoscope* 2002;112:2129–40.
19. Jeon GA, Lee JS, Patel V, et al. Global gene expression profiles of human head and neck squamous carcinoma cell lines. *Int J Cancer* 2004;112:249–58.
20. Boukamp P, Popp S, Altmeyer S, et al. Sustained nontumorigenic phenotype correlates with a largely stable chromosome content during long-term culture of the human keratinocyte line HaCaT. *Genes Chromosomes Cancer* 1997;19:201–14.
21. Sriuranpong V, Park JI, Amornphimoltham P, Patel V, Nelkin BD, Gutkind JS. Epidermal growth factor receptor-independent constitutive activation of STAT3 in head and neck squamous cell carcinoma is mediated by the autocrine/paracrine stimulation of the interleukin 6/gp130 cytokine system. *Cancer Res* 2003;63:2948–56.
22. Wendel HG, De Stanchina E, Fridman JS, et al. Survival signalling by Akt and eIF4E in oncogenesis and cancer therapy. *Nature* 2004;428:332–7.
23. Patel V, Senderowicz AM, Pinto D, Jr., et al. Flavopiridol, a novel cyclin-dependent kinase inhibitor, suppresses the growth of head and neck squamous cell carcinomas by inducing apoptosis. *J Clin Invest* 1998;102:1674–81.
24. Dykes DJ, Harrison SD, Jr., Mayo JG, Griswold DP, Jr. Excision assay for initial evaluation of antitumor drug activity in mice bearing human tumor xenografts. *J Natl Cancer Inst* 1992;84:528–30.
25. Plowman J, DJ Dykes M, Hollingshead L, Simpson-Herren, Alley MC. Human tumor xenograft models in NCI drug development. In: Teicher B, editor. *Anticancer drug development guide: preclinical screening, clinical trials, and approval*. Totowa (NJ): Humana Press, Inc.; 1997. p. 101–30.
26. Fiebig HH, Berger DP, Winterhalter BR, Plowman J. *In vitro* and *in vivo* evaluation of US-NCI compounds in human tumor xenografts. *Cancer Treat Rev* 1990;17:109–17.
27. Sodhi A, Montaner S, Patel V, et al. Akt plays a central role in sarcomagenesis induced by Kaposi's sarcoma herpesvirus-encoded G protein-coupled receptor. *Proc Natl Acad Sci U S A* 2004;101:4821–6.
28. Charafe-Jauffret E, Tarpin C, Bardou VJ, et al. Immunophenotypic analysis of inflammatory breast cancers: identification of an 'inflammatory signature'. *J Pathol* 2004;202:265–73.
29. Vlahos CJ, Matter WF, Hui KY, Brown RF. A specific inhibitor of phosphatidylinositol 3-kinase, 2-(4-morpholinyl)-8-phenyl-4H-1-benzopyran-4-one (LY294002). *J Biol Chem* 1994;269:5241–8.
30. Pomerantz RG, Grandis JR. The epidermal growth factor receptor signaling network in head and neck carcinogenesis and implications for targeted therapy. *Semin Oncol* 2004;31:734–43.
31. Davies SP, Reddy H, Caivano M, Cohen P. Specificity and mechanism of action of some commonly used protein kinase inhibitors. *Biochem J* 2000;351:95–105.
32. Sato S, Fujita N, Tsuruo T. Interference with PDK1-Akt survival signaling pathway by UCN-01 (7-hydroxystaurosporine). *Oncogene* 2002;21:1727–38.
33. Sabers CJ, Martin MM, Brunn GJ, et al. Isolation of a protein target of the FKBP12-rapamycin complex in mammalian cells. *J Biol Chem* 1995;270:815–22.
34. Gingras AC, Kennedy SG, O'Leary MA, Sonenberg N, Hay N. 4E-BP1, a repressor of mRNA translation, is phosphorylated and inactivated by the Akt(PKB) signaling pathway. *Genes Dev* 1998;12:502–13.
35. Robbins KT, Vu TP, Diaz A, Varki NM. Growth effects of tamoxifen and estradiol on laryngeal carcinoma cell lines. *Arch Otolaryngol Head Neck Surg* 1994;120:1261–6.
36. Takechi T, Fujioka A, Matsushima E, Fukushima M. Enhancement of the antitumor activity of 5-fluorouracil (5-FU) by inhibiting dihydropyrimidine dehydrogenase activity (DPD) using 5-chloro-2,4-dihydroxypyridine (CDHP) in human tumour cells. *Eur J Cancer* 2002;38:1271–7.
37. Abdulkarim B, Sabri S, Deutsch E, et al. Antiviral agent Cidofovir restores p53 function and enhances the radiosensitivity in HPV-associated cancers. *Oncogene* 2002;21:2334–46.
38. Pomerantz RG, Grandis JR. The role of epidermal growth factor receptor in head and neck squamous cell carcinoma. *Curr Oncol Rep* 2003;5:140–6.
39. Morello S, Olivero M, Aimettili M, et al. MET receptor is overexpressed but not mutated in oral squamous cell carcinomas. *J Cell Physiol* 2001;189:285–90.
40. Redon R, Muller D, Caulee K, Wanherdrick K, Abecassis J, du Manoir S. A simple specific pattern of chromosomal aberrations at early stages of head and neck squamous cell carcinomas: PIK3CA but not p63 gene as a likely target of 3q26-qter gains. *Cancer Res* 2001;61:4122–9.
41. Chang AA, Van Waes C. Nuclear factor- κ B as a common target and activator of oncogenes in head and neck squamous cell carcinoma. *Adv Otorhinolaryngol* 2005;62:92–102.
42. Song JI, Grandis JR. STAT signaling in head and neck cancer. *Oncogene* 2000;19:2489–95.
43. Nikitakis NG, Siavash H, Sauk JJ. Targeting the STAT pathway in head and neck cancer: recent advances and future prospects. *Curr Cancer Drug Targets* 2004;4:637–51.
44. Ford AC, Grandis JR. Targeting epidermal growth factor receptor in head and neck cancer. *Head Neck* 2003;25:62–73.
45. Cohen EE. Novel therapeutic targets in squamous cell carcinoma of the head and neck. *Semin Oncol* 2004;31:755–68.
46. Chan S. Targeting the mammalian target of rapamycin (mTOR): a new approach to treating cancer. *Br J Cancer* 2004;91:1420–4.
47. Hidalgo M, Rowinsky EK. The rapamycin-sensitive signal transduction pathway as a target for cancer therapy. *Oncogene* 2000;19:6680–6.
48. Guba M, von Breitenbuch P, Steinbauer M, et al. Rapamycin inhibits primary and metastatic tumor growth by antiangiogenesis: involvement of vascular endothelial growth factor. *Nat Med* 2002;8:128–35.
49. Majumder PK, Febbo PG, Bikoff R, et al. mTOR inhibition reverses Akt-dependent prostate intraepithelial neoplasia through regulation of apoptotic and HIF-1-dependent pathways. *Nat Med* 2004;10:594–601.
50. Abraham RT. TOR signaling: an odyssey from cellular stress to the cell growth machinery. *Curr Biol* 2005;15:R139–41.
51. Thomas SM, Grandis JR. Pharmacokinetic and pharmacodynamic properties of EGFR inhibitors under clinical investigation. *Cancer Treat Rev* 2004;30:255–68.
52. Hynes NE, Lane HA. ERBB receptors and cancer: the complexity of targeted inhibitors. *Nat Rev Cancer* 2005;5:341–54.
53. Sulis ML, Parsons R. PTEN: from pathology to biology. *Trends Cell Biol* 2003;13:478–83.
54. Li J, Yen C, Liaw D, et al. PTEN, a putative protein tyrosine phosphatase gene mutated in human brain, breast, and prostate cancer. *Science* 1997;275:1943–7.
55. Spicer J, Ashworth A. LKB1 kinase: master and commander of metabolism and polarity. *Curr Biol* 2004;14:R383–5.
56. Mak BC, Yeung RS. The tuberous sclerosis complex genes in tumor development. *Cancer Invest* 2004;22:588–603.
57. Lee JI, Soria JC, Hassan KA, et al. Loss of PTEN expression as a prognostic marker for tongue cancer. *Arch Otolaryngol Head Neck Surg* 2001;127:1441–5.
58. Raymond E, Alexandre J, Faivre S, et al. Safety and pharmacokinetics of escalated doses of weekly intravenous infusion of CCI-779, a novel mTOR inhibitor, in patients with cancer. *J Clin Oncol* 2004;22:2336–47.
59. Boni JP, Leister C, Bender G, et al. Population pharmacokinetics of CCI-779: correlations to safety and pharmacogenomic responses in patients with advanced renal cancer. *Clin Pharmacol Ther* 2005;77:76–89.
60. Sawyers CL. Will mTOR inhibitors make it as cancer drugs? *Cancer Cell* 2003;4:343–8.

Cancer Research

The Journal of Cancer Research (1916–1930) | The American Journal of Cancer (1931–1940)

Mammalian Target of Rapamycin, a Molecular Target in Squamous Cell Carcinomas of the Head and Neck

Panomwat Amornphimoltham, Vyomesh Patel, Akrit Sodhi, et al.

Cancer Res 2005;65:9953-9961.

Updated version Access the most recent version of this article at:
<http://cancerres.aacrjournals.org/content/65/21/9953>

Cited articles This article cites 57 articles, 13 of which you can access for free at:
<http://cancerres.aacrjournals.org/content/65/21/9953.full#ref-list-1>

Citing articles This article has been cited by 32 HighWire-hosted articles. Access the articles at:
<http://cancerres.aacrjournals.org/content/65/21/9953.full#related-urls>

E-mail alerts [Sign up to receive free email-alerts](#) related to this article or journal.

Reprints and Subscriptions To order reprints of this article or to subscribe to the journal, contact the AACR Publications Department at pubs@aacr.org.

Permissions To request permission to re-use all or part of this article, use this link
<http://cancerres.aacrjournals.org/content/65/21/9953>.
Click on "Request Permissions" which will take you to the Copyright Clearance Center's (CCC) Rightslink site.